

Influence of construction loading on deflections in reinforced concrete slabs

R. L. Vollum and N. Afshar

Imperial College London

This paper describes and analyses a series of tests on one-way spanning slabs, which were carried out at Imperial College London to investigate the influence of peak construction loads on long-term tension stiffening and slab deflections. The work was carried out to investigate the validity of conclusions drawn from the first author's back analysis of deflection data in the Cardington in situ concrete building, which suggested that long-term deflections in slabs could be governed by short-term construction and in-service loads. An improved method is proposed for taking account of the effect of peak construction loads on long-term slab deflections. The method is shown to be more accurate than the rigorous method in Concrete Society Report TR58 which is based on the first authors' analysis of slab deflections at Cardington.

NOTATION

| | |
|------------------|-----------------------------------------------------------------------------------------------------|
| E_{ct} | elastic modulus for concrete at time t |
| E_{ceff} | effective elastic modulus for concrete, $= E_{ct}/(1 + \phi(t_i, t))$ |
| E_{LT} | equivalent effective elastic modulus for concrete loaded in stages |
| f_{ct} | concrete tensile strength |
| k | damage coefficient, $= \sqrt[3]{\beta f_{ct}/w}$ |
| M | applied bending moment |
| $M_{conc\ mean}$ | mean bending moment resisted by concrete in tension between cracks, $= M - T_{sm}(d - x_m/3)$ |
| M_{peak} | bending moment under peak construction load |
| M_{perm} | bending moment under permanent load |
| M_f | cracking moment |
| ΔM | $M_{peak} - M_{perm}$ |
| $1/r_1$ | curvature in uncracked section |
| $1/r_2$ | curvature in fully cracked section |
| $1/r_m$ | mean curvature |
| T_{sm} | mean tensile force in reinforcement between cracks, $= A_s E_s \epsilon_{sm}$ |
| w | uniformly distributed load |
| x_m | mean depth to neutral axis between cracks |
| β | coefficient used in calculation of ζ |

| | |
|------------------|--------------------------------------------------------------------|
| ϵ_{sh} | free shrinkage strain |
| ϵ_{sm} | mean strain in reinforcement |
| $\phi(t_i, t)$ | creep coefficient at time t for concrete loaded at time t_i |
| ζ, ζ^* | coefficients used in calculation of mean curvature |

Introduction

Analysis of deflection data from the Cardington in situ concrete building¹ suggested that long-term slab deflections can be governed by early-age striking or peak construction loads from casting slabs above. At that time, there were no suitable laboratory data available to validate the analytical model derived from back analysis of the Cardington^{1,2} data. The current test programme was designed to rectify this omission. Vollum's method¹⁻³ for accounting for construction loading in deflection calculations is a refinement of the moment–curvature approach given in Eurocode 2.⁴ The method was subsequently adopted in Concrete Society Technical Report TR58,⁵ where it is referred to as the 'rigorous method'. It is useful to review the approach adopted in Eurocode 2⁴ for predicting long-term deflections, and the loss of tension stiffening with time, before considering the influence of construction loading. Curvatures increase with time in reinforced concrete flexural members owing to the combined effects of creep, shrinkage and loss of tension stiffening with time. In Eurocode 2,⁴ the mean curvature in cracked members is given by

Department of Civil and Environmental Engineering, Imperial College London, South Kensington Campus, London, UK

(MACR-D-08-00009) Paper received 21 December 2007; last revised 32 March 2008; accepted 6 June 2008

$$1/r_m = \xi 1/r_2 + (1 - \xi) 1/r_1 \quad (1)$$

where

$$\xi = 1 - \beta(M_r/M)^2 \quad (2)$$

$1/r_1$ and $1/r_2$ are the curvatures of uncracked and full sections respectively including shrinkage and M_r is the cracking moment. The coefficient β in equation (2) takes account of loss of tension stiffening with time owing to additional internal- and macro-cracking under sustained load. Eurocode 2⁴ states that β should be taken as 1 for short-term loading and 0.5 for long-term loading, but does not define the variation in β with time.

Recently, Beeby and Scott⁶ carried out a series of relatively short-term tests (up to around 100 days) on tension members which showed that the residual tensile force resisted by cracked concrete reduces to its long-term value within a few weeks of loading. The specimens were first loaded around 28 days after casting. They found that the long-term mean residual tensile stress in the concrete between cracks was around half the instantaneous value after first cracking. Beeby and Scott⁶ concluded that tension stiffening was largely lost owing to additional cracking and internal damage under sustained load as the tensile strength of concrete reduces to around 70% of its instantaneous value under sustained loading. Beeby and Scott's⁶ data suggest that the time function describing the rate of loss of tension stiffening in tension specimens is approximately

$$\beta(t) = -0.12 \log_{10}(t) + 0.65 \quad \text{with} \quad 0.5 \leq \beta(t) \leq 1.0 \quad (3)$$

where $\beta(t)$ is a function of time and t is the time in days from first cracking.

Beeby and Scott⁶ carried out some exploratory slab tests which suggested that tension stiffening is lost rapidly in slabs but at a slower rate than in tension specimens. As a result of these tests Beeby and Scott⁶ suggested that β should be taken as 0.5 in most cases in equation (2). Vollum⁷ also analysed deflection data from various slabs tested by others in the laboratory under constant loading and concluded that β typically reduced from 1 to around 0.7, in cracked members, between 1 and 2 days after first loading. Some aspects of Vollum's⁷ analysis were speculative as creep and shrinkage strains were typically measured in control specimens which had a significantly smaller notional size than the slabs. It was therefore difficult accurately to assess the contributions of creep and shrinkage to deflection in the first few days after loading.

Influence of construction loads on long-term slab deflections

Relatively short-term peaks in slab loads can arise during the construction of multi-storey buildings from

casting slabs above or in service as illustrated in Fig. 1, which was derived from back prop forces measured at St George Wharf.⁸ It is assumed in Fig. 1 that the slab carries its self-weight after striking. The main problems in predicting deflections under loading histories similar to that shown in Fig. 1 are to determine (a) the influence of short-term peak loads on the long-term residual tension stiffening under sustained load and (b) the deflection after repeated unloading and reloading.

The Cardington deflection data¹⁻³ are particularly useful for assessing the influence of construction loading on slab deflections as the loading on the first six floors was measured during construction and the permanent loading was the same at all floors. Variations in construction loading, concrete strengths and reinforcement between floors led to significant variations in deflection between floors. Analysis of the Cardington data^{1,2,7} showed that the measured deflections under the permanent load, at a specific location, varied almost linearly with the minimum value of a coefficient k , which was defined as

$$k = \sqrt{\beta f_{ct}/w} \quad (4)$$

where f_{ct} and w were evaluated at either striking, under the peak construction load or under the permanent load. The minimum value of k corresponds to the loading stage which induces the worst cracking. It was assumed that the interpolation coefficient ξ corresponding to k_{min} governs long-term deflections as cracking is irreversible. The long-term deflections were shown to be governed by striking or peak construction loads provided that β was taken as less than 0.86 in k_{strike} and k_{peak} . Hossain and Vollum² obtained good estimates of long-term deflections at Cardington using (a) an incremental analytical procedure with $\beta = 0.7$ and (b) a single step analysis with $\beta = 0.5$. Hossain and Vollum² adopted Rotilio's⁹ procedure for calculating curvatures after unloading in their incremental procedure for calculating deflection. Rotilio⁹ assumed that the short-term unloading response follows a line that intersects the response of the uncracked section at a moment equal and opposite to that immediately before unloading. A drawback with Rotilio's⁹ approach is that it needs to be implemented in an incremental procedure

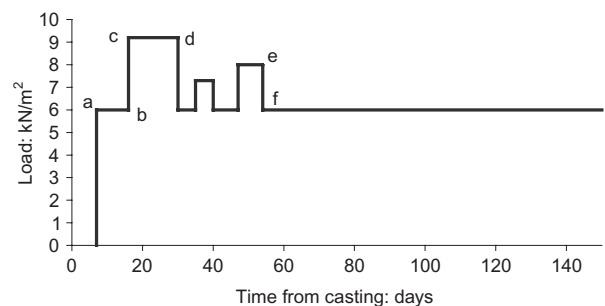


Fig. 1. Load history from casting slabs above for two levels of backprops

such as that devised by Hossain and Vollum.² In practice, it is more convenient to calculate deflections corresponding to load histories such as that in Fig. 1 in a single step procedure in conjunction with a suitably modified concrete tensile strength and creep coefficient. The slab tests described in the current paper were designed to enable the development of improved methods for deflection prediction under load histories such as those presented Fig. 1.

Slab tests

A series of six simply supported one-way spanning slabs were tested in the Concrete Structures Laboratory at Imperial College to determine the influence of short-term construction loads on long-term slab deflections. The slabs measured 500 mm wide by 3600 mm long by 150 mm thick and were reinforced with 3T10 bars as shown in Fig. 2. The span of 3300 mm was chosen to satisfy the span-to-effective depth ratios in Eurocode 2,⁴ which are intended to limit the total deflection to span/250 under a quasi-permanent load equal to half the design ultimate load. Equation (7.16a) in Eurocode 2⁴ gives a maximum permissible span of 3537 mm for the authors' slabs with $f_{ck} = 30$ MPa.

The slabs were loaded at their third points with straps attached to one or two concrete blocks with additional steel kentledge as required, which gave an almost constant moment within the central third of the slab. The ratio of the maximum to minimum moments in the central third of the beam varied between 1.03 and 1.04 in the tests. Slabs S1–S3 were first loaded 9 days after casting. Constant loads were applied to slabs S1 and S2 throughout the test. Slab S3 was loaded for 5 days with a peak load equal to 1.4 times the permanent load, which was the same as for slab S2. Slabs S4–S6 were first loaded with their self-weight at 7 days and the quasi-permanent load was applied at 34 days. In between, a peak construction load was applied to slabs S4 and S5 at 13 days and sustained for a period of 4 days. The peak load applied to S4 equalled the permanent load which

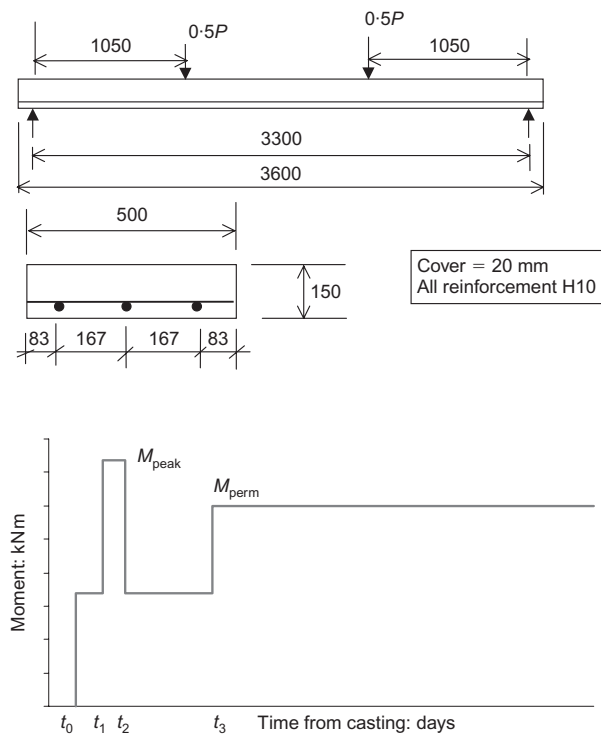


Fig. 2. Details of test specimens

was notionally identical in slabs S2–S6. Full details of the load histories are given in Table 1, which should be read in conjunction with Fig. 2.

Long-term deflections are governed by factors including

- the reinforcement stress under the quasi-permanent (sustained) loading,
- the ratio between the peak construction moment and the quasi-permanent moment (M_{peak}/M_{perm}) and
- the ratio between the peak moment and the cracking moment (M_{peak}/M_r).

These data are summarised in Table 2, which also gives the maximum deflections measured in the tests. Table 2 also shows that the ratio between M_{perm} and the

Table 1. Loading history for slabs S1–S6

| Specimen | S1 | S2 | S3 | S4 | S5 | S6 |
|----------------------------|------|-------|-------|------|-------|------|
| Self weight: kN | 7.43 | 7.00 | 7.02 | 6.87 | 6.93 | 6.69 |
| P_{peak} : kN | — | — | 16.88 | 8.54 | 12.39 | — |
| P_{perm} : kN | 8.21 | 10.26 | 10.49 | 8.54 | 8.30 | 8.47 |
| M_{swt} : kNm | — | — | — | 2.44 | 2.46 | 2.38 |
| M_{peak} : kNm | — | — | 11.35 | 6.92 | 8.97 | — |
| M_{perm} : kNm | 6.95 | 7.87 | 7.99 | 6.92 | 6.82 | 6.82 |
| t_0 (self-weight) | 9 | 9 | 9 | 7 | 7 | 7 |
| t_1 (apply P_{peak}) | — | — | 9 | 13 | 13 | — |
| t_2 (remove P_{peak}) | — | — | 14 | 17 | 17 | — |
| t_3 (apply P_{perm}) | 9 | 9 | 14 | 34 | 34 | 34 |

Note: All times in days from casting.

Table 2. Summary of test data

| Slab | S1 | S2 | S3 | S4 | S5 | S6 |
|-----------------------------------|-------|-------|-------|-------|-------|-------|
| f_{perm} : MPa | 253 | 287 | 291 | 254 | 250 | 250 |
| $M_{\text{perm}}/M_{\text{Rd}}$ | 0.57 | 0.65 | 0.66 | 0.57 | 0.56 | 0.56 |
| $M_{\text{peak}}/M_{\text{perm}}$ | 1.00 | 1.00 | 1.42 | 1.00 | 1.32 | 1.00 |
| $M_{\text{peak}}/M_{\text{r}}$ | 1.02 | 1.15 | 1.66 | 1.21 | 1.57 | 1.19 |
| Time $^{\psi}$ t_4 | 100* | 100* | 100* | 126 | 126 | 126 |
| Deflection at t_4 | 11.14 | 15.94 | 21.61 | 15.1 | 17.75 | 14.3 |
| Normalised deflection at t_4 | 0.70 | 1.00 | 1.36 | 1.06 | 1.24 | 1.00 |
| Time $^{\psi}$ at t_5 | — | — | — | 330 | 330 | 330 |
| Deflection at t_5 | — | — | — | 19.01 | 20.86 | 18.41 |
| Normalised deflection at t_5 | — | — | — | 1.03 | 1.13 | 1.00 |

Notes: $^{\psi}$ All times in days from first loading, All deflections in mm, *End of test.

design ultimate moment of resistance M_{Rd} varied between 0.56 and 0.65, which is typical for slabs in buildings.

Instrumentation

Deflections were measured at the centre of the slab and adjacent to the loading points. Strains were measured with a 150 mm Demec gauge along one edge of each slab (a) near the level of the reinforcement, (b) at mid-height and (c) just below the top surface of the slab. In situ strains were also measured with a Demec gauge in the top surface of each slab, parallel and perpendicular to the direction of span. Strains were also measured in the top and bottom surfaces of the slabs with electrical resistance strain gauges.

Concrete material properties

The slabs were cast in two batches of three, approximately 5 months apart, from ready-mix concrete with a target 28 day cylinder strength of 30 MPa. The flexural and splitting strengths of the concrete were determined from control specimens cured in air and water. The depth of the beams used in the flexural tests was chosen to be 150 mm to eliminate the influence on flexural strength of differences in section depth between the control specimens and slabs. The resulting tensile strengths are given in Table 3 which also gives tensile strengths derived from the concrete compressive strength using the equations given in Eurocode 2.⁴

Creep and shrinkage strains were measured in 4×10 inches (10.16×25.40 cm) control cylinders and derived from strain measurements in the slabs. The in situ shrinkage strain was calculated as follows

$$\varepsilon_{\text{sh}} = (\varepsilon_t + \nu \varepsilon_l) / (1 + \nu) \quad (5)$$

where

ε_l is the longitudinal strain

ε_t is the transverse strain

ν is Poisson's ratio

Figures 3 and 4 show the increments in shrinkage

Table 3. Concrete material properties

| Specimen | S1–S3 | | S4–S6 | |
|------------------------------|-------|------|-------|------|
| Age: days | 7.0 | 28.0 | 13.0 | 34.0 |
| f_{cu} : MPa | 21.8 | 32.1 | 31.2 | 37.9 |
| E : GPa | 31.2 | 32.6 | 26.6 | 26.7 |
| f_{ct} (watercured) | 2.1 | 2.8 | 2.8 | 3.2 |
| f_{ct} (aircured) | — | — | 2.1 | 2.5 |
| f_{ct} (Eurocode 2) | 2.0 | 2.6 | 2.6 | 2.9 |
| f_{tl} (watercured) | 3.1 | — | 3.3 | — |
| f_{tl} (aircured) | 2.4 | — | 2.4 | — |
| f_{tl} (Eurocode2) | 2.9 | 3.8 | 3.7 | 4.2 |
| f_{ct} M1 | 2.9 | — | 3.1 | — |
| f_{ct} M2 | 3.0 | — | 2.4 | — |
| f_{ct} M3 (used) | 3.5 | — | 2.9 | 2.9 |

Note: All concrete strengths in MPa

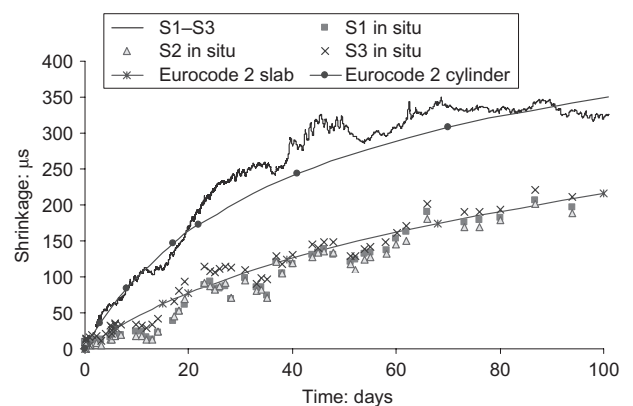


Fig. 3. Shrinkage strains in slabs S1 to S3

strain measured in the slabs and control cylinders from first loading. The figures also show the increments in shrinkage strains predicted by Eurocode 2⁴ from first loading. Fig. 3 shows that the shrinkage strains measured in tests S1–S3 were similar to those predicted by Eurocode 2. Fig. 4 shows that the shrinkage strains measured in slabs S4–S6 increased more rapidly than predicted by Eurocode 2 and that no significant increase in shrinkage occurred after 200 days.

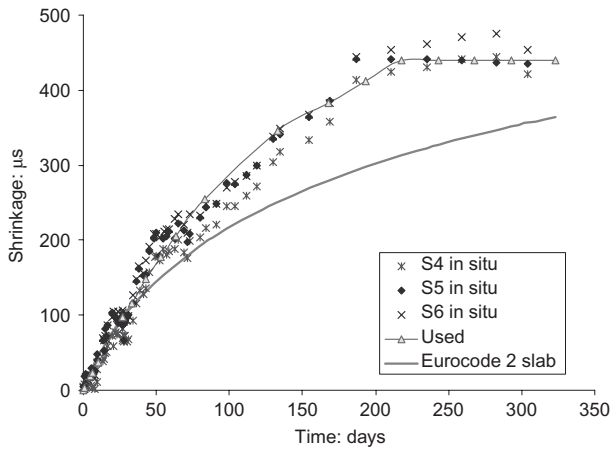
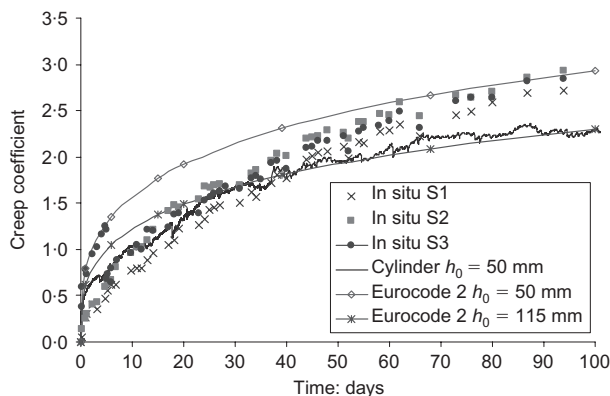
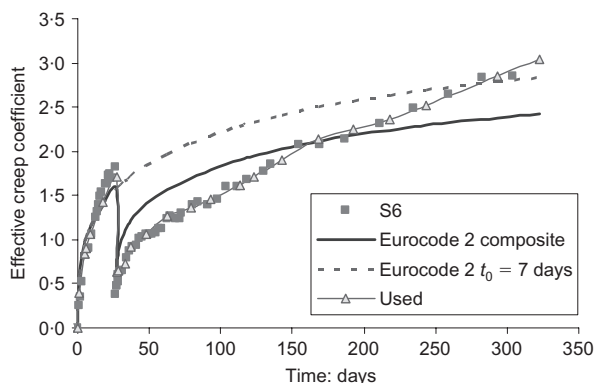


Fig. 4. Shrinkage strains in slabs S4 to S6

Creep coefficients were estimated from strain measurements in the control cylinders and from changes in curvature derived from strain measurements in the uncracked sections of the slabs adjacent to the supports. The in situ creep coefficients were derived in a section analysis which compensated for the influences of shrinkage and internal restraint from the reinforcement. The creep coefficients in Figs 5 and 6 were calculated in terms of instantaneous strains corresponding to the in situ elastic modulus of the slabs at first loading.


 Fig. 5. Creep coefficients for slabs S1 to S3 ($E_c(t_0) = 30$ GPa)

 Fig. 6. Creep coefficients for slab S6 ($E_c(t_0) = 23.4$ GPa)

The resulting creep coefficients are shown in Fig. 5 for tests S1–S3 and in Fig. 6 for test S6. The figures also give the creep coefficients predicted by Eurocode 2⁴ which were scaled by $E_c(t_0)/E_{c28}$ where E_{c28} is the elastic modulus at 28 days. It is interesting to note that the creep coefficients measured in situ were slightly greater than those measured in the control cylinders which was unexpected. The rate of increase of the in situ creep coefficients in slabs S1–S3 was also significantly greater after 30 days than predicted by Eurocode 2.⁴ The current authors attribute the difference in creep behaviour between the control cylinders and slabs to the slabs being in flexure unlike the control cylinders which were in compression. The creep coefficient is greater in flexure in compression because it is increased by creep in tension, which is greater than in compression. Neville¹⁰ also points out that the decrease in the rate of creep with time is much less pronounced in tension than compression because the increase in tensile strength with time is less.

Determination of in situ cracking moment

It was anticipated that the effective flexural strength of the concrete in the slabs would lie between the splitting and flexural strengths as the flexural strength of reinforced concrete is reduced by shrinkage owing to the internal restraint provided by reinforcement. Three approaches were used to estimate the in situ flexural strength of the concrete in the slabs. In method M1, the in situ strength was estimated by reducing the flexural strength of the control beams by the tensile stress induced in the slabs by restrained shrinkage which was estimated as follows

$$f_{ctsh}(t) = E_s \varepsilon_{sh}(t_s) S_1 (h - x_1) / I_1 + A_s E_s \varepsilon_{sh}(t_s) / (A_c (1 + m\rho)) \quad (6)$$

where $\rho = A_s/A_c$, m is the effective modular ratio E_s/E_{ceff} and t_s is the time at onset of shrinkage.

In method M2, the flexural strength was estimated from the moment at which the moment-curvature response of the slabs became non-linear. In method M3, the flexural strength was chosen to give a good fit between the instantaneous measured deflections and those predicted by Eurocode 2 with $\beta = 1$. Method M3 is illustrated in Figs 7 and 8, which show that curvatures are underestimated around the cracking moment if the flexural strength is chosen to give the best overall estimate of the measured instantaneous curvatures. In reality, tension stiffening is lost progressively as cracks form successively as the moment increases. It is unclear from the present tests to what extent Eurocode 2⁴ takes this into account as strain data are unavailable to relate the loss of tension stiffening in the tests to the development of cracks during loading. It appears that the Eurocode 2⁴ moment–

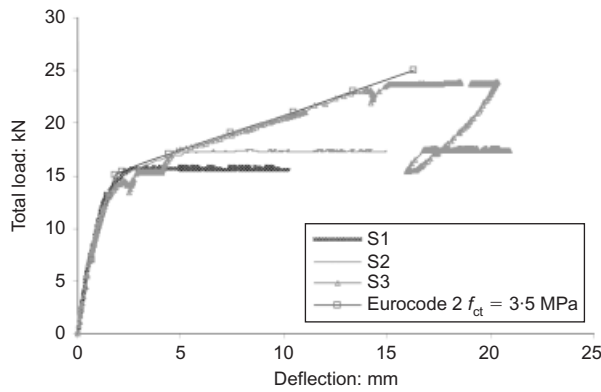


Fig. 7. Deflection plotted against load in slabs S1 to S3

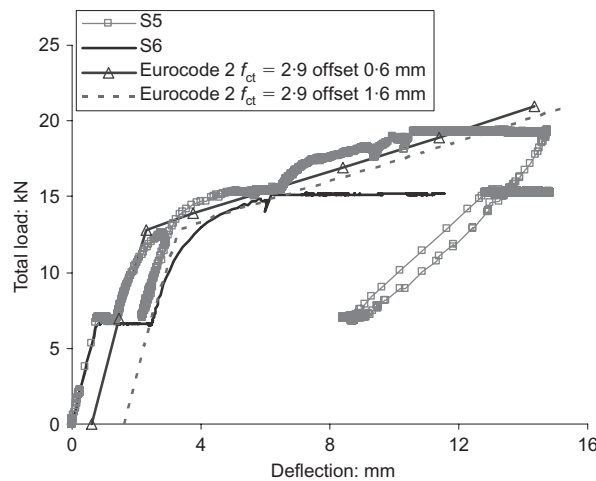


Fig. 8. Deflection plotted against load in slabs S4 to S6

curvature relationship may underestimate the short-term tension stiffening effect provided by cracked concrete below the neutral axis if the moment at first cracking is used in equation (2). This conclusion is consistent with the common practice of using the mean concrete rather than minimum tensile strength to determine a best estimate of likely deflections.

The concrete flexural strengths corresponding to methods M1–M3 are listed in Table 3, which includes the measured flexural and splitting strengths for comparison. The tensile strengths obtained with M3 were adopted in the analysis of the slab data described in this article as they give the best estimates of deflection in conjunction with Eurocode 2.⁴ The concrete tensile strength given by M3 was the same for slabs S4 and S6. This was unexpected as slab S1 was loaded to cracking at 13 days whereas slab S6 was loaded to cracking at 34 days when the tensile strength of the control specimens was greater as shown in Table 3.

Results

The influence of peak construction loads on deflection can be seen by comparing the deflections in Table 2 and

the mid-span curvatures in Figs 9 and 10. It is apparent that the peak construction load increased deflections significantly in slabs S3 (compared to S2) and S5 (compared to S6) at 100 days, and that the difference in deflections between slabs S5 and S6 reduced with time.

The rate of loss of tension stiffening with time is significant in the calculation of long-term deflections under load histories similar to Fig. 1 as long-term deflections can be governed by the residual tension stiffening remaining immediately before unloading from the peak load. Slab tests S1, S2 and S6 provide data on the rate of loss of tension stiffening in slabs under a uniform sustained load. Tests S3–S5 provide data on the residual tension stiffening remaining after unloading from a short-term peak load. The mean moment resisted by the concrete in tension between cracks was estimated in the test slabs with the following equation

$$M_{\text{conc mean}} = M - T_{\text{sm}}(d - x_{\text{m}}/3) \quad (7)$$

where M is the applied moment, $T_{\text{sm}} = A_s E_s \epsilon_{\text{sm}}$, ϵ_{sm} is the mean strain in the concrete at the level of the reinforcement and x_{m} is the mean value of the depth to the neutral axis both of which were determined from the Demec strain readings.

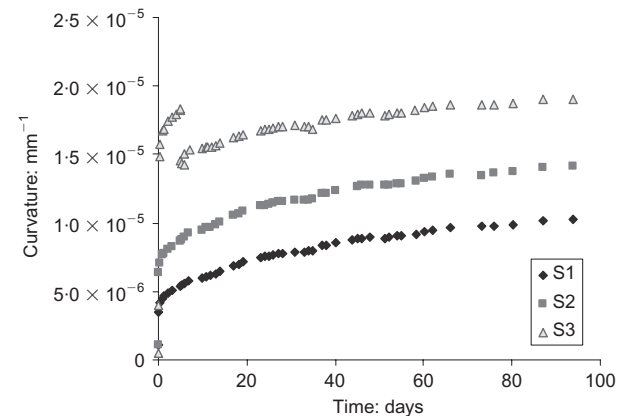


Fig. 9. Comparison between curvatures in central third of slabs S1–S3

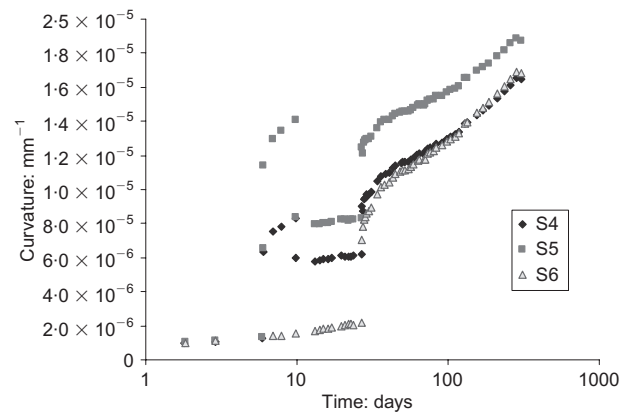


Fig. 10. Comparison between curvatures in central third of slabs S4–S6

The development of deflection with time depends significantly on the rate of loss in the tension stiffening moment with time which is governed by β in equation (2). According to the Eurocode 2⁴ moment–curvature model, the mean residual moment resisted by the concrete between cracks is given by

$$M_{\text{conc mean}} = (1 - \zeta)M_{\text{conc l}} = \beta(M_r/M)^2 M_{\text{conc l}} \quad (8)$$

where $M_{\text{conc l}}$ is the moment resisted by concrete in tension in an uncracked section, which is close to the total bending moment M in lightly reinforced sections such as slabs. The coefficient β in equation (2) can be estimated by assuming $M_{\text{conc l}} = M$ and rearranging equation (8) as follows

$$\beta_t = (M_{\text{conc mean}}/M_r)(M(t)/M_r) \quad (9)$$

where $M(t)$ is the bending moment at time t . The variation in β with $\log(\text{time})$ was estimated with equation (9) with $M_{\text{conc mean}}$ from equation (7) assuming $M_{\text{conc l}} = M$. The resulting values of β are plotted against $\log_{10}(\text{time})$ in Fig. 11(a) and against time in Fig. 11(b). It can be seen that β reduced at a similar rate with time in all the slabs. The discontinuity in the values of β in slabs S3 and S5 arises as β was calculated under the current rather than peak moment. In all cases, β reduced linearly in $\log_{10}(\text{time})$ for around 12

days from first loading or the duration of the peak load if less. Thereafter, β reduced much more slowly as shown in Fig. 11(b) for the duration of the measurements presented which is up to one year. It appears that β reduced more rapidly after the shrinkage strain plateaued at around 200 days.

A number of different mechanisms are responsible for the long-term loss of tension stiffening in slabs. It seems likely that the rapid loss of tension stiffening after first cracking is attributable to internal cracking of the concrete under sustained load as proposed by Beeby and Scott.⁶ The subsequent gradual loss of tension stiffening appears to be caused by relaxation of the concrete in tension between the cracks owing to creep. The effect of creep is counter-balanced in part by shrinkage, which induces tensile stresses in the concrete between the cracks owing to the restraining effect of the reinforcement. These suppositions are supported by the observation that β increased more rapidly after the shrinkage plateaued at 200 days. Fig. 11(a) also shows that β reduced at a significantly slower rate in the slabs than in the tension specimens of Beeby and Scott.⁶

The authors' tests were designed primarily to investigate the short-term loss of tension stiffening under peak construction loads and no change is suggested to the long-term value of β of 0.5 in Eurocode 2.⁴ Regression analysis showed that β reduced as follows in slab S6 which was typical

$$\beta(t) = -0.0364 \ln(t) + 0.8279 \quad 0 = t = 12 \text{ days} \quad (10a)$$

$$\beta(t) = -0.0008t + 0.7327 \quad t > 12 \text{ days} \quad (10b)$$

with $0.5 \leq \beta(t) \leq 1.0$.

The accuracy of equation (8) was investigated by plotting $M_{\text{conc mean}}/M_r$ in slabs S1–S6 against M/M_r four days after the application of the peak construction load when β was around 0.8. Fig. 12 shows that the experimental values of $M_{\text{conc mean}}/M_r$ given by equation (7) compare very well with the theoretical values given by equation (8) derived from Eurocode 2⁴ with $\beta = 0.8$.

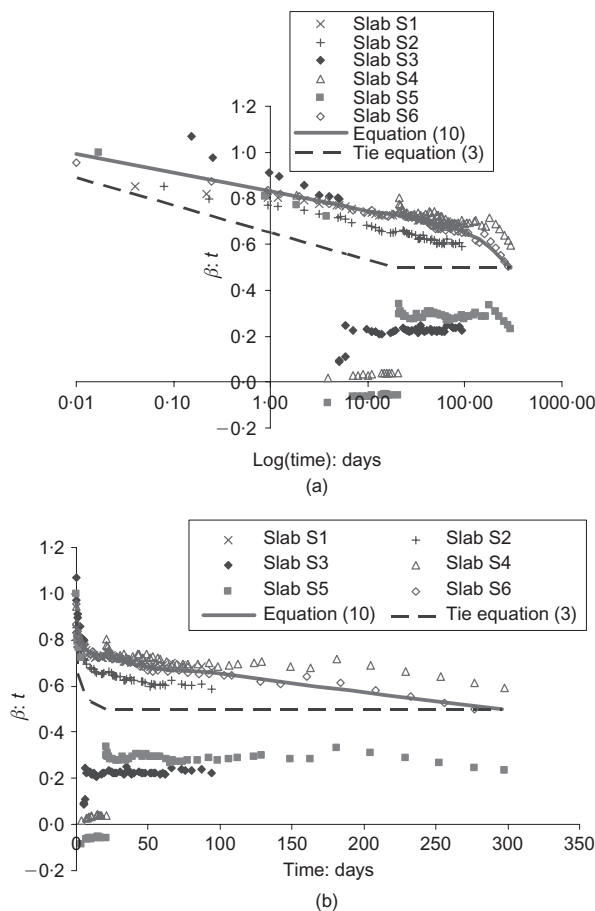


Fig. 11. (a) Variation in β with $\log(\text{time})$ in slabs S1–S6; (b) Variation in β with time in slabs S1–S6

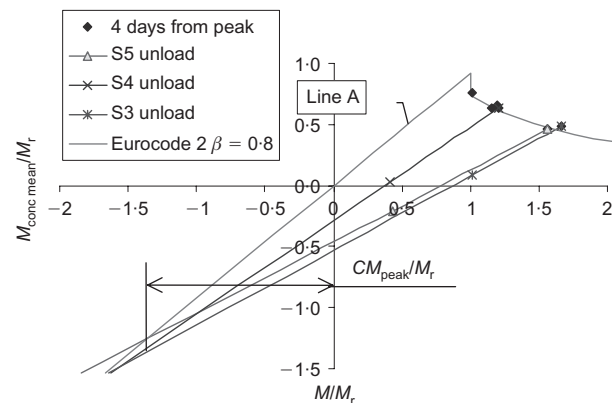


Fig. 12. Relationship between $M_{\text{conc mean}}/M_r$ and M/M_r in slabs S1–S6

Influence of short term peak loads on tension stiffening

Vollum *et al.*^{1,2} showed that deflections at Cardington varied linearly with the coefficient k_{\min} defined in equation (4). They went on to propose that the influence of peak construction loads could be accounted for in deflection calculations by using a modified concrete tensile strength given by

$$f_{ctmod} = k_{\min} w \quad (11)$$

where k_{\min} = minimum value of $k = \sqrt{\beta f_{ct}/w}$ evaluated during construction and subsequently.

Vollum *et al.*¹⁻³ attributed the linear relationship between k and deflection to the fact that Eurocode 2⁴ predicts long-term deflections in cracked slabs with given dimensions, reinforcement and loading to vary almost linearly with f_{ct} . The current research shows this explanation is overly simplistic and presents a more thorough explanation, which accounts for the effects of unloading. The starting point is to rearrange equation (2) as below

$$1/r_m = 1/r_2 - \beta(M_r/M)^2(1/r_2 - 1/r_1) \quad (12)$$

It follows that the mean curvatures in a set of geometrically identical slabs vary linearly at any given time with $\beta(M_r/M)^2$ or k^2 for a given M (i.e. $1/r_1$ and $1/r_2$). Analysis shows that k typically varies almost linearly with k^2 for cracked slabs which explains the observed linear relationship between k and deflections predicted with Eurocode 2⁴ under constant load and varying concrete tensile strength. The data from slabs S1–S6 were analysed to determine if, at any given time, there was a linear relationship between $(M_{perm\ S1}/M_{perm})1/r_m$ and (a) $(M_r/M)^2$ and (b) M_r/M as anticipated from the first author's analysis of the Cardington deflection data. The curvatures $1/r_m$ were normalised by the ratio $M_{perm\ S1}/M_{perm}$ (where M_{perm} is the mid-span moment in the slab under consideration under the permanent load and S1 denotes slab S1) as the permanent load varied between the tests as shown in Table 2. The normalisation is justified as the curvatures $1/r_1$ and $1/r_2$ are almost proportional to the applied moment as the curvature induced by shrinkage is relatively small. The results of a typical analysis are shown in Figs 13 and 14, which show that there was a linear relationship between $(M_{perm\ S1}/M_{perm})1/r_m$ and both $(M_r/M_{peak})^2$ and M_r/M_{peak} in slabs S1 to S6 at 93 days when the permanent load was removed from slabs S1–S3.

The reason for the linear relationship between $(M_{perm\ S1}/M_{perm})1/r_m$ and $(M_r/M)^2$ in slabs that have been unloaded requires further explanation as the unloading line does not pass through the origin. In this case, the mean curvature can be expressed as

$$1/r_m = \zeta^* 1/r_2 + (1 - \zeta^*) 1/r_1 \quad (13)$$

where ζ^* depends on the previous load history. Fig. 7 shows that the deflection reduced almost linearly in

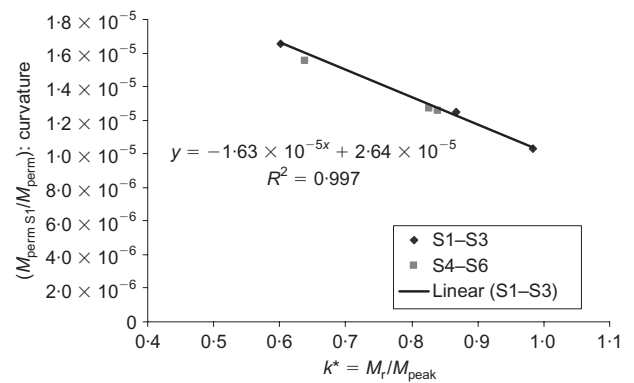


Fig. 13. Relationship between normalised curvatures and M_r/M_{peak} for slabs S1–S6 at 93 days

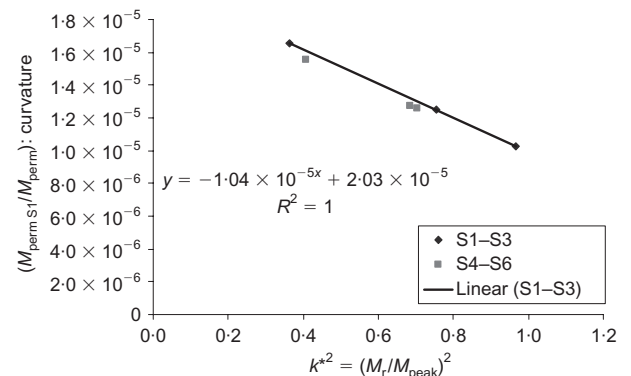


Fig. 14. Relationship between normalised curvatures and $(M_r/M_{peak})^2$ for slabs S1–S6 at 93 days

slab S3 after unloading from the peak construction load. If M_{conc1}/M is assumed to be 1, which is reasonable for lightly reinforced members like slabs, consideration of Fig. 12 shows that the mean tension stiffening moment after unloading is given by

$$M_{conc\ mean} = (1 - \zeta^*)M_{perm} = M_{peak}(1 - \zeta_{peak}) - \Delta M(1 - \zeta_{peak}/(1 + C)) \quad (14)$$

where $\Delta M = M_{peak} - M_{perm}$ and $-CM_{peak}/M_r$ is the horizontal ordinate at which the unloading line intersects line A in Fig. 12.

Rotilio⁸ method⁸ can be shown to be equivalent to assuming $C = 1$ in equation (14). The coefficient C in equation (14) was evaluated for slabs S3 to S5 by equating the measured mean tension stiffening moment after unloading to that given by equation (14) using the graphical procedure illustrated in Fig. 12. The corresponding values of C were 1.0 for S3, 1.3 for S4 and 0.9 for S5 with a mean of 1.1. The mean measured and predicted tension stiffening moments $M_{conc\ mean}$ given by equations (8) and (14) respectively are compared for slabs S3, S5 and S6 in Figs 15(a) to (c), which show a remarkable agreement between the measured and predicted values. Rearranging equation (14) gives

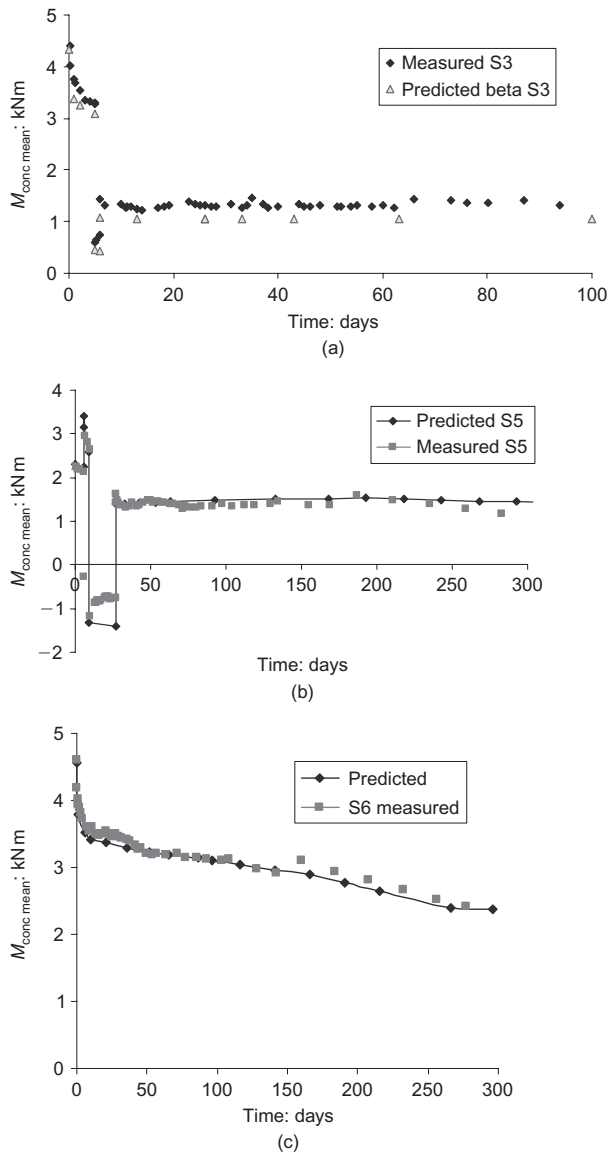


Fig. 15. (a) Comparison between measured and predicted $M_{conc mean}$ for slab S3; (b) Comparison between measured and predicted $M_{conc mean}$ for slab S5; (c). Comparison between measured and predicted $M_{conc mean}$ for slab S6

$$\zeta^* = \zeta_{peak}(1 + CM_{peak}/M_{perm})/(1 + C) \quad (15)$$

Analysis shows that the curvatures given by equation (13) are relatively insensitive to the value used for C in the calculation of ζ^* in equation (15) and it is suggested that C is taken as 1 throughout as implicitly assumed in the Rotilio⁸ method.

Equation (13) implies that the normalised curvatures $((M_{perm S1}/M_{perm})1/r_m)$ and corresponding mid-span deflections should vary linearly with $1 - \zeta^*$ at any given time. This has been investigated for slabs S1 to S6 and the results are given in Fig. 16, which shows a remarkably linear relationship between $1 - \zeta^*$ and curvature in slabs S1 to S6 at 93 days as predicted. Analysis shows that the linear relationship is virtually independent of the value of C used to define the slope of the unloading line in equation (15).

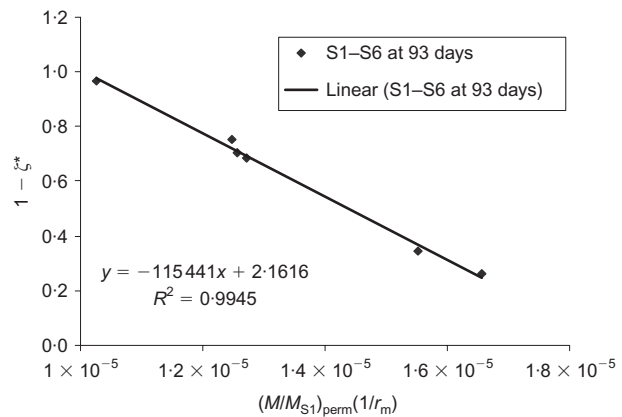


Fig. 16. Relationship between normalised curvatures at 90 days and $1 - \zeta^*$ for slabs S1–S6 at 93 days

Rigorous method for deflection prediction in Concrete Society Technical Report TR58

Concrete Society Technical Report TR58⁵ uses a single step method, based on the recommendations of Vollum *et al.*,^{1–3} to predict curvatures owing to load histories as presented in Fig. 2. The mean curvature is calculated with equation (1) in conjunction with equation (2) and modified values for the concrete tensile strength and effective elastic modulus. TR58⁵ uses the following equation, based on the theory of superposition, to calculate a modified effective elastic modulus for concrete

$$E_{LT} = \sum W_i / (W_1/E_{ceff1} + W_2/E_{ceff2} + W_3/E_{ceff3} + \dots) \quad (16)$$

where W_i is the load increment at time t_i and $E_{ceff} = E_{ct}/(1 + \phi(t_i, t))$ where t_i is the age at application of W_i and t is the age at which deflections are required.

TR58⁵ uses equation (11) to modify the concrete tensile strength to account for cracking during construction and under peak loads. It is recommended in TR58⁵ that β is taken as 0.5 in equation (2) as tension stiffening is lost rapidly after first loading. The method in TR58⁵ neglects the residual increase in curvature Δ^*/r_m that remains after unloading from peak loads (see Fig. 8). This omission was justified in the development of the method by observing that the effect of neglecting Δ^*/r_m in the calculation of the long-term curvature under w_{perm} is largely compensated by overestimating the loss in tension stiffening under the peak construction load.

Proposed method for deflection prediction

It is proposed that the rigorous method for deflection prediction in TR58⁵ should be modified by calculating the interpolation coefficient in equation (1) correspond-

ing to the peak construction load with equation (15) with $C = 1$. In practice, ζ_{peak} can be calculated under the applied loading using f_{ctmod} (see equation (11)) and $M_{\text{peak}}/M_{\text{perm}}$ can be approximated as $w_{\text{peak}}/w_{\text{perm}}$ for uniformly loaded slabs. The coefficient β used in the calculation of ζ_{peak} can be estimated with equation (10) if the duration of the peak construction load is known or, more conservatively, β can be taken as 0.7 for peak construction loads of up to five weeks duration. It is suggested that the interpolation coefficient ζ should be taken as the greatest of either ζ_{frequent} (where ζ_{frequent} is calculated under the frequent load with $\beta = 0.5$) or ζ^* in the calculation of long-term deflections.

Validation of proposed method

The accuracy of the proposed method for deflection prediction has been evaluated by comparing measured and predicted deflections in slabs S1–S6. Curvatures were calculated with methods outlined below.

- TR58 A: TR58⁵ with concrete material properties derived with Eurocode 2 from the concrete compressive strength with the concrete tensile strength taken as the flexural strength.
- TR58 B: TR58⁵ with concrete material properties derived with Eurocode 2 from the concrete compressive strength with the concrete tensile strength taken as the splitting strength.
- TR58 C: TR58⁵ with the measured concrete material properties.
- Proposed: Proposed method with the measured concrete material properties and the experimental values of β .

The creep and shrinkage values used in TR58 C and the proposed method were derived from the equations of the lines of best fit to the mean in situ data shown in Figs 3–6. Measured creep coefficients were used to determine the curvatures under the peak construction loads in slabs S3, S4 and S5 but the increase in creep owing to the application of the peak construction load was neglected in the calculation of curvatures after the removal of the peak construction load. In reality, the in situ creep coefficients were greater in slabs S4 and S5 than S6 as the additional creep under the peak construction load was not fully recovered on unloading as shown in Fig. 17. Despite this the measured long-term curvatures within the constant moment region of slabs S4 and S6 are very similar as shown in Fig. 10, even though the curvature was greater in the uncracked sections, adjacent to the supports, of slab S4 than S6. The reason for this is probably related to the fact that the effective creep coefficient is greater in the uncracked regions of the slab than in the cracked regions where tension is relieved in the concrete by cracking. In practice, compressive creep coefficients are usually used in deflection calculations. The present work suggests that

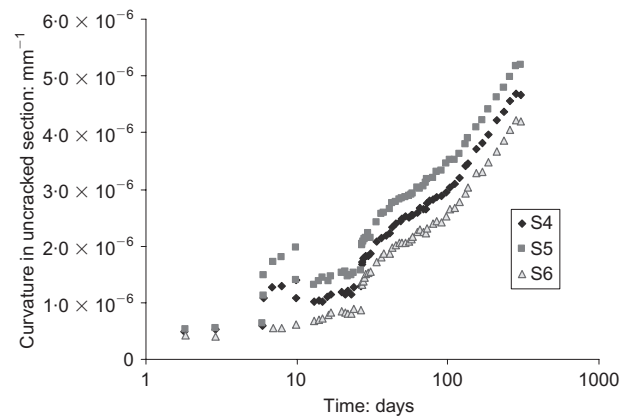


Fig. 17. Comparison between curvatures in uncracked section of slabs S4 and S6

this can lead to an underestimate of deflection in lightly loaded slabs with significant tension stiffening.

The measured and predicted mean mid-span curvatures are compared in Figs 18(a)–(f), which show that the proposed method gives significantly more realistic estimates of curvature in slabs S3 to S5 under the peak construction load and subsequently than the rigorous method in TR58.⁵ Furthermore, it can be seen that the curvature predictions are significantly improved when measured material properties are used, with curvatures being particularly sensitive to the concrete tensile strength, which was unexpectedly low in tests S4–S6 for unknown reasons. It can be seen that deflections were overestimated in slabs S1 and S2 if the concrete tensile strengths were calculated in terms of the compressive strength using Eurocode 2. Conversely, deflections were significantly underestimated in slab S6 if the concrete tensile strength was taken as the flexural strength given by Eurocode 2 at 34 days when the permanent load was applied and cracking occurred.

Conclusions

It has been demonstrated that tension stiffening is lost rapidly after cracking in flexural members but less rapidly than measured by Beeby and Scott⁶ in tension members. It is shown that long-term deflections can be governed by short-term peaks in construction loading as suggested by analysis of deflection data from Cardington.^{1,2} A modification is proposed to the Eurocode 2⁴ moment–curvature model to calculate the residual tension stiffening moment remaining in members after unloading from short-term peak loads. Expressions are developed to calculate the variation in time of the coefficient β in the Eurocode 2⁴ moment–curvature relationship. A refinement is proposed to the rigorous method for deflection prediction in Concrete Society Technical report 58,⁵ which is shown to give improved estimates of deflection after the removal of the peak

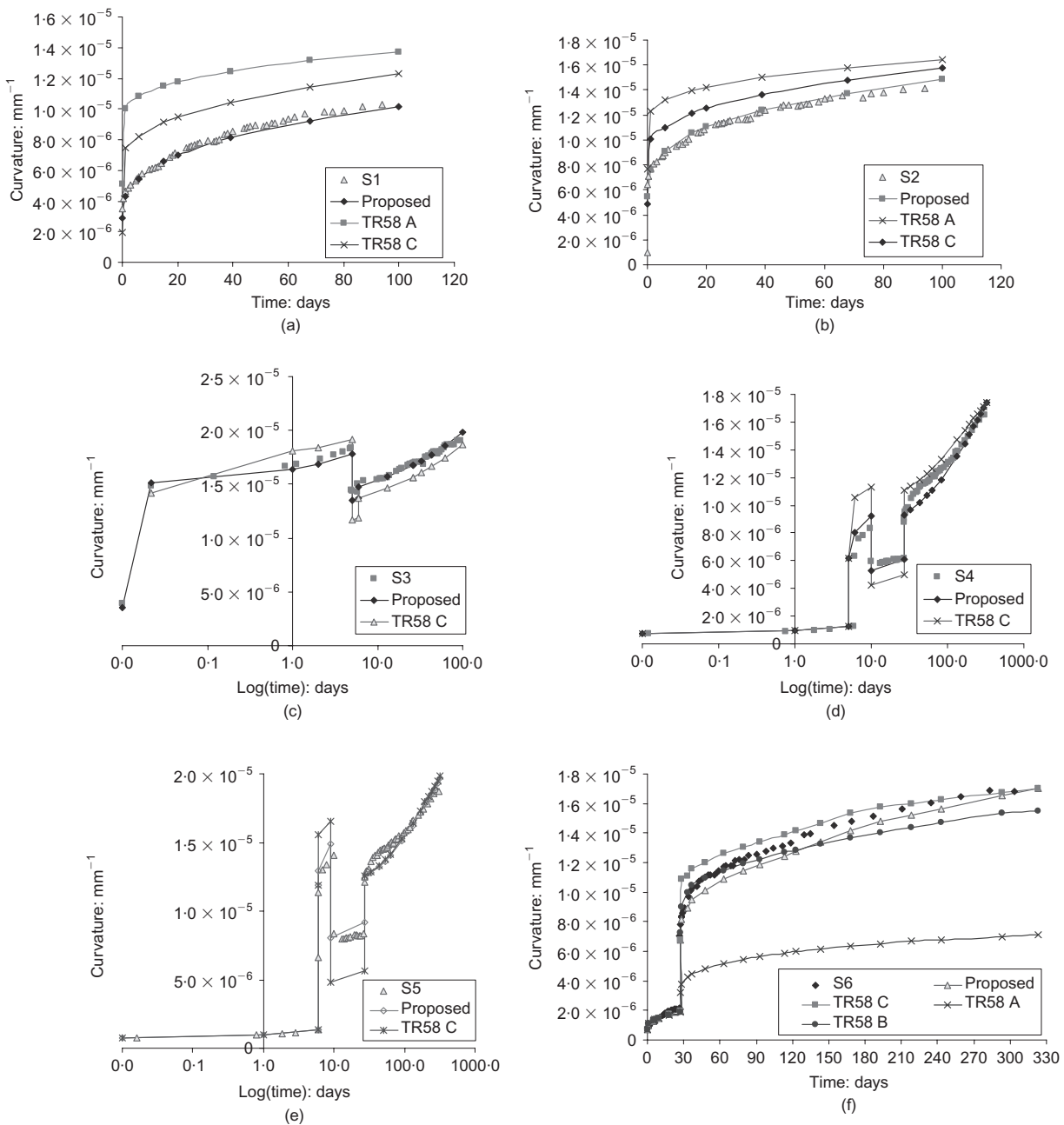


Fig. 18. (a) Comparison of measured and predicted curvatures in slab S1; (b) Comparison of measured and predicted curvatures in slab S2; (c) Comparison of measured and predicted curvatures in slab S3; (d) Comparison of measured and predicted curvatures in slab S4; (e) Comparison of measured and predicted curvatures in slab S5; (f) Comparison of measured and predicted curvatures in slab S6

construction load. The analysis of the test data shows that deflections can vary significantly from values predicted with material properties derived in terms of the concrete compressive strength. It is shown that deflections in slabs can be particularly sensitive to the concrete tensile strength, which is uncertain at the design stage. It is noteworthy that the final deflections in all the slabs were greater than span/250 (13.2 mm) even though the slabs complied with the span-to-effective depth ratios in Eurocode 2.⁴

References

1. VOLLUM R. L., MOSS R. M. and HOSSAIN T. R. Slab deflections in the Cardington in-situ concrete frame building. *Magazine of Concrete Research*, 2002, **54**, No. 1, 23–34.
2. HOSSAIN T. R. and VOLLUM R. L. Prediction of slab deflections and validation against Cardington data. *Proceedings of the Institution of Civil Engineers, Structures and Building*, 2002, **152**, No. 3, 235–248.
3. VOLLUM R. L. and HOSSAIN T. R. Are existing span-to-depth rules conservative for flat slabs? *Magazine of Concrete Research*, 2002, **54**, No. 6, 411–421.
4. BRITISH STANDARDS INSTITUTION. Eurocode 2: *Design of Con-*

- crete Structures: Part 1-1: General Rules and Rules for Buildings. BSI, London, 2004. BS EN 1992-1-1:2004
5. CONCRETE SOCIETY. *Deflections in Concrete Beams and Slabs*. The Concrete Society, Camberley, 2005. Technical Report 58.
 6. BEEBY A. W. and SCOTT R. H. Tension stiffening of concrete, behaviour of tension zones in reinforced concrete including time dependent effects. *Supplementary Information*. The Concrete Society, Camberley, 2004. Technical Report 59.
 7. VOLLUM R. L. Influences of shrinkage and construction loading on loss of tension stiffening in slabs. *Magazine of Concrete Research*, 2002, **54**, No. 4, 273–282.
 8. VOLLUM R. L. Investigation into backprop forces and deflections at St George Wharf. *Magazine of Concrete Research*, 2003, **55**, No. 5, 449–460.
 9. ROTILIO J.-D. Moment–curvature relationship. *XIII FIP Congress and Exhibition, The Netherlands*, 1998.
 10. NEVILLE A. M. *Properties of Concrete*, 4th edn. Longman, Harlow, 1995.

Discussion contributions on this paper should reach the editor by 1 August 2009